



# Contrasting nickel and manganese accumulation and localization in New Caledonian Cunoniaceae

Antony van der Ent · Yohan Pillon · Bruno Fogliani · Vidiro Gei · Tanguy Jaffré · Peter D. Erskine · Guillaume Echevarria · Kathryn M. Spiers · Adrian L. D. Paul · Sandrine Isnard

Received: 19 January 2022 / Accepted: 12 March 2022 / Published online: 4 April 2022  
© The Author(s) 2022

## Abstract

**Purpose** The Cunoniaceae are a major component of the New Caledonian flora with 91 endemic species that are highly unusual in that multiple metals are hyperaccumulated in different species. This makes it an ideal model system for studying the nature of the hyperaccumulation phenomenon.

**Methods** X-ray fluorescence spectroscopy (XRF) scanning of all herbarium collections of the Cunoniaceae was undertaken at the Herbarium of New Caledonia to reveal incidences of nickel (Ni) and manganese (Mn) accumulation. Following on, the Mn hyperaccumulating *P. reticulata* and the Ni hyperaccumulating *P. xaragurensis* were selected for detailed

follow-up investigations using synchrotron-based X-ray fluorescence microscopy (XFM).

**Results** The systematic XRF screening of herbarium specimens showed that numerous species have high foliar Mn and Ni with species either accumulating Ni or Mn, but not both elements simultaneously. Soil ‘extractable’ Mn and Ni concentrations associated with *Pancheria reticulata* and *P. xaragurensis* greatly varies between the species. The XFM data shows that *P. reticulata* has a distinctive distribution pattern with Mn concentrated in large hypodermal cells. This contrasts with *P. xaragurensis* where Ni was mainly localized in and around the epidermis, and hypodermal cells were not observed.

Responsible Editor: Fangjie Zhao.

**Supplementary Information** The online version contains supplementary material available at <https://doi.org/10.1007/s11104-022-05388-3>.

A. van der Ent · V. Gei · P. D. Erskine · A. L. D. Paul  
Centre for Mined Land Rehabilitation, Sustainable Minerals Institute, The University of Queensland, Brisbane, QLD 4072, Australia

A. van der Ent (✉) · G. Echevarria  
Université de Lorraine, INRAE, Laboratoire Sols et Environnement, Vandoeuvre-les-Nancy, France  
e-mail: a.vanderent@uq.edu.au

Y. Pillon  
LSTM, IRD, INRAE, CIRAD, Institut Agro, Université Montpellier, Montpellier, France

B. Fogliani  
Institut des Sciences Exactes et Appliquées, Université de la Nouvelle-Calédonie, BR R4 98851, Nouméa, Nouvelle-Calédonie, France

T. Jaffré · S. Isnard  
AMAP, Université Montpellier, IRD, CIRAD, CNRS, INRAE, Montpellier, France

T. Jaffré  
AMAP, IRD, Herbar de Nouvelle-Calédonie, Nouméa, New Caledonia, France

K. M. Spiers  
Photon Science, Deutsches Elektronen-Synchrotron DESY, Hamburg, Germany

**Conclusions** Manganese and Ni accumulation are differently localized in *Pancheria* species growing on ultramafic soils, which is not explained by contrasting soils conditions, but represents different ecophysiological adaptations.

**Keywords** Cunoniaceae · Elemental mapping · Hyperaccumulator · Manganese · Nickel · New Caledonia · Ultramafic soils · XRF

## Introduction

Hyperaccumulators are a group of rare plants that are capable of concentrating exceptionally high levels of specific metals or metalloids into their living tissues (Baker and Brooks 1989; Reeves 2003; van der Ent et al. 2013). Hyperaccumulator plants have evolved specific root uptake and foliar sequestration mechanisms to attain these very high concentrations of metals/metalloids in their shoots (Baker 1981; Krämer 2010; Pollard et al. 2002). The hyperaccumulation phenomenon is mainly known for nickel (Ni), and Ni hyperaccumulators represent ~70% of the ~700 hyperaccumulator species recorded to date (Reeves et al. 2017). Manganese hyperaccumulators are unusual among other trace metal(oid) hyperaccumulators, because Mn concentrations are relatively high in most soils and this element is essential for normal plant growth (Loneragan 1988). Until recently, there were only 42 known Mn hyperaccumulator species worldwide (Manara et al. 2020; Reeves et al. 2017), but it now appears that Mn hyperaccumulation has been overlooked with the discovery of 74 Mn hyperaccumulator taxa in New Caledonia (Gei et al. 2020a) and 51 Mn hyperaccumulator taxa in Sabah, Malaysia (van der Ent et al. 2019b). Elemental analysis of leaf tissue samples has typically been undertaken via Atomic Absorption Spectrophotometry (AAS) or Inductively Coupled Plasma-Atomic Emission Spectroscopy (ICP-AES) (e.g. Fernando et al. 2009; Jaffré 1979; Kelly et al. 1975; Reeves et al. 1996), after mineral acid digestion of dry foliar samples. This process is time-consuming and inherently destructive, but handheld X-ray fluorescence spectroscopy (XRF) devices have enabled non-destructive analysis of massive numbers of herbarium specimens (Gei et al. 2020b; van der Ent et al. 2019a, b). This new XRF-based approach has already considerably increased the number of

known Mn hyperaccumulating species, suggesting that this trait was largely under-reported (Gei et al. 2020b; van der Ent et al. 2019b).

Hyperaccumulators differ from non-hyperaccumulators in their enhanced root uptake, efficient long distance transport mechanisms from roots to leaves and efficient compartmentalization of metal ions in vacuoles and/or the apoplast of foliar cells (Sharma et al. 2016). The exact localization of metals within the leaf is of central significance because it might interfere with metabolic processes such as photosynthesis. Investigations based on X-ray fluorescence techniques (including synchrotron-based X-ray fluorescence microscopy or XFM and nuclear proton-beam or microPIXE) have been applied to study the Mn localization for several known Mn hyperaccumulator genera (*Gossia*, *Viotia*, *Grevillea*, *Denhamia*, *Garcinia*). In contrast to other hyperaccumulators (such as for Ni, Zn) examined to date, where the metal is preferentially compartmentalized in the vacuoles of epidermal cells, or in the interstitial space of leaves, Mn hyperaccumulators exhibit diverse detoxification ecophysologies (Fernando et al. 2008a, 2012, 2007). Manganese has variously been found to be primary localized in photosynthetic (palisade mesophyll cells), or lower to non-photosynthetic (epidermal and hypodermal cells, spongy mesophyll cells) tissues or in both tissue types (Fernando et al. 2008a, 2012, 2007).

Two areas of the world are especially renowned for their richness in metal hyperaccumulator plants: Cuba (Reeves et al. 1996, 1999; Belloeil et al. 2021) and New Caledonia (Gei et al. 2020b; Jaffré et al. 2013). These islands both have large surface areas of ultramafic outcrops where most of the metal hyperaccumulators (particularly those for Ni) have been reported. Soils derived from ultramafic rocks pose strong edaphic pressures to plant growth and are typically characterised by a highly characteristic vegetation assembly (Kazakou et al. 2008; Proctor 2003), and this is particularly noteworthy in New Caledonia (Isnard et al. 2016). New Caledonia is globally recognized for its extremely high levels of diversity of the vascular flora with a remarkable endemism at the species-level (74.7%, Morat et al. 2012; Munzinger et al. 2022. [continuingly updated]) and at the higher taxonomic level (Pillon et al. 2017). A major component of this flora is the Cunoniaceae, a woody plant family of 27 genera and ~335 species predominantly occurring in the Southern Hemisphere (Bradford

et al. 2004). The Cunoniaceae is most diverse in New Caledonia with 91 endemic species (Hopkins et al. 2014) and it was one of the first tropical plant families in which Ni hyperaccumulation has been reported, particularly in the genus *Geissois* (Jaffré 1980; Jaffré et al. 2013; Pillon et al. 2014). The recent screening of the Herbarium of New Caledonia (NOU) with XRF technology (Gei et al. 2020b) has confirmed that metal (hyper)accumulation (particularly for Mn and Ni) is common in this family. The Cunoniaceae are a rare example of a plant family where multiple metals are hyperaccumulated in different taxa, and this makes this taxonomic group an ideal model system to increase the understanding of the evolution, adaptations and ecophysiology underlying the accumulation of different transition metals.

In our current work, we re-analysed the raw XRF data previously acquired from the New Caledonian Cunoniaceae using an improved quantification model, and then focussed on two taxa: the Mn hyperaccumulator *Pancheria reticulata* and the Ni hyperaccumulator *Pancheria xaragurensis*, for further investigations. We used synchrotron-based X-ray fluorescence microscopy (XFM) to determine the tissue-level distribution of Mn, Ni, and other elements. We also analysed field collected plant tissue samples of both taxa and their associated soil chemistry. The aim of this study is to use the Cunoniaceae as a model system for studying the nature of the hyperaccumulation phenomenon and to identify shared mechanisms or differences in the accumulation of the two metals in two contrasting species of *Pancheria*.

## Materials and methods

### Herbarium XRF screening of Cunoniaceae herbarium specimens

The Cunoniaceae in New Caledonia have a strong preference for ultramafic substrates (mainly occurring on Ferralsols, at middle and high altitude and on hydromorphic soils at lower altitude) with 66 of the 91 endemic species recorded on ultramafic soils, and 25 species are nearly always restricted to non-ultramafic substrates (Hopkins et al. 2014). A total of 2519 specimens of Cunoniaceae from New Caledonia, representing all 91 native species (Suppl Info), were analysed at the Herbarium of New Caledonia (NOU). The classification

here follows the recent taxonomic treatment by Hopkins et al. (2014) with the transfer of *Weinmannia* species to the genus *Pterophylla* (Pillon et al. 2021a), hybrid taxa were excluded, and infraspecies were not distinguished. The methods used have been described in detail elsewhere (Gei et al. 2020b). A handheld XRF device (Thermo Fisher Scientific Niton XL3t 950 GOLDD+) was used to measure the elemental concentrations of Ni and Mn in the leaves of the herbarium specimens. Following completion of the earlier extensive herbarium XRF screening study at the Herbarium of New Caledonia (NOU) (Gei et al. 2020b), the calibration model for XRF measurements was further improved (Paul et al. 2020a). This revised calibration (which has an improved regression fit of  $R^2$  0.97 for Mn) was used in this study to determine the concentrations of Mn in the Cunoniaceae family with greater accuracy. For each species and element, the median rather than the mean was used, as means are more sensitive to extreme values, which are common in this dataset and could not be calculated for many species when most specimens had values below the limit of detection (LOD for Mn  $455 \mu\text{g g}^{-1}$  and for Ni  $107 \mu\text{g g}^{-1}$ ).

### Collection of *Pancheria* samples for bulk chemical analyses

Two species of *Pancheria* were selected for the follow-up investigations: *Pancheria reticulata* Guillaumin, which is a Mn hyperaccumulator, and *Pancheria xaragurensis* H.C. Hopkins & Pillon, which is a Ni hyperaccumulator (Fig. 1). *Pancheria reticulata* is a New Caledonia endemic shrub that sparsely occurs on Grande Terre, exclusively growing on ultramafic soils, on the northern mining massif of the west coast, but also in the south. It is found in shrubland (locally called “maquis”) and occasionally in forest at mid and high altitude (600–1200 m asl). The samples (n=10 biological replicates) of *P. reticulata* were collected from a single population located at Mont Mou ( $22^{\circ}4'32.58''\text{S}$ ,  $166^{\circ}20'23.94''\text{E}$ , altitude 680 m) in the southern massif, in open ligno-herbaceous maquis on a strongly weathered Ferralsol. *Pancheria xaragurensis* is a shrub endemic to the south-east of Grande Terre in the region of Thio and Côte Oubliée. It is found in low altitude scrubland exclusively on ultramafic soils, especially along waterways (Hopkins et al. 2014; Hopkins and Pillon 2011). The samples of *P. xaragurensis* (n=5 biological replicates)

**Fig. 1** *Pancheria reticulata* and *P. xaragurensis* in the native habitat. Panel **a** *P. reticulata* at Mont Mou in New Caledonia, branches with leaves and infructescences. **b** *P. reticulata* cut bark of stem exhibiting orange colour **c** *P. xaragurensis* at Thio along Tô De river



were collected from a single population at Thio on alluvial terrace, in a bushy maquis along the Tô De river (21°41'11.96"S, 166°20'14.35"E, altitude 10 m). In addition (for chemical analysis only), two other *Pancheria* species were collected to confirm the veracity of the herbarium XRF analysis (Suppl Table 2). These are: *P. engleriana* Schltr., which is a Ni hyperaccumulator and collected at Mont Mou (22° 4'26.92"S, 166°20'32.28"E, altitude 700 m) and *Pancheria multijuga* Guillaumin ex H.C.Hopkins & J. Bradford, which is a Mn hyperaccumulator collected in shrubland on Mont Humboldt (21°52'39.26"S, 166°24'52.29", altitude 1300 m). Plant tissue samples (n=2 biological replicates for *P. engleriana* and n=1 biological replicate for *P. multijuga*): young/apical leaves, old/basal leaves, branches (woody stems), wood, bark tissue including phloem, fine roots, for elemental analysis were oven dried at 70 °C for five days. The bark and wood samples were obtained by stripping it from branches using a sharp stainless-steel knife. The samples were weighed and ground to a fine powder and subsequently acid digested with 4 mL HNO<sub>3</sub> (70%) in a digestion microwave (Milestone, model Start D) using a 45-min programme. The samples were brought to volume (40 mL) with ultrapure water before analysis using Inductively

coupled plasma atomic emission spectroscopy (ICP-AES) with a Thermo Scientific iCAP 7400 instrument as described previously (Paul et al. 2020a, b).

#### Collection and chemical analysis of soils associated with *P. reticulata* and *P. xaragurensis*

The soil samples were collected from around the base (e.g., within 25 cm of the trunk) of 10 different *P. reticulata* plants growing on Mont Mou and of 5 different *P. xaragurensis* plants growing at Tô De River, from a depth of 0–15 cm, after removing the litter. The soil samples were air-dried and sieved (<2 mm). Soil pH was measured in a 1:2.5 soil:water slurry after 2 h of shaking using a glass electrode (Ionode using a 'soil probe'). Exchangeable transition elements were analysed by extraction using 0.1 M Sr(NO<sub>3</sub>)<sub>2</sub> solution in a soil:solution ratio of 1:4 (10 g soil: 40 mL solution) and 2 h shaking time, while phytoavailable trace elements were extracted in diethylenetriamine penta-acetic acid (DTPA-extractant) solution adapted from (Lindsay and Norvell 1978) as described previously (Paul et al. 2020a, b) and then analysed using ICP-AES as for the plant material samples.



### Collection and processing of *P. reticulata* and *P. xaragurensis* specimens for XFM

Due to the remote access to the field locations in New Caledonia and logistical challenges with travel to Germany, we were unable to analyse fresh-hydrated specimens for *P. reticulata*. Hence, specimens were freeze-dried (as described below) so that they could be kept until the synchrotron XFM experiment took place. However, we were able to collect specimens of *P. xaragurensis* and bring them in fresh-hydrated state to Germany (within two days after collection) for the synchrotron XFM experiment in a subsequent session. The *P. reticulata* specimens (leaves) were obtained by cutting leaf portions with a razor blade and immediately shock-frozen (employing the metal mirror method) to affect rapid freezing of the tissues to limit cellular damage by the formation of ice crystals (Fernando et al. 2013). The specimens were stored in a liquid nitrogen vapour cryogenic container (at least  $-190\text{ }^{\circ}\text{C}$ ). The specimens were cut (30- $\mu\text{m}$  slices) with a cryo-microtome (Leica CM1950 Clinical Cryostat) at  $-30\text{ }^{\circ}\text{C}$  and finally freeze-dried (in a Thermoline freeze-dryer). The lyophilization process begun at  $-196\text{ }^{\circ}\text{C}$  with the frozen specimens in thermal contact with a large stainless-steel block cooled in liquid nitrogen in the freeze-dryer and then progressed slowly by increasing the temperature in  $5\text{ }^{\circ}\text{C}$  increments until reaching room temperature (the whole process took four days). The freeze-dried specimens were then stored in a desiccator until XFM analyses, as described below. The sample preparation methods may conceivably influence the localization of certain elements, depending on their distribution or form prior to sublimation. However, a careful slow freeze-drying process does not lead to structural changes or elemental distribution, even at the cellular scale (Tylko et al. 2007a, b; Wang et al. 2013).

### X-ray fluorescence microscopy (XFM) of *P. reticulata* and *P. xaragurensis*

The X-ray fluorescence microscopy (XFM) experiment was performed at the PETRA III (Deutsches Elektronen-Synchrotron; DESY) at beamline P06 that has a cryogenically cooled double-crystal monochromator with Si(111) crystals and a K/B mirror system that focusses a beam of  $10^{11}$  photon/s down to 300 nm size in the energy range 5–21 keV (Schroer

et al. 2010). The data for *P. reticulata* was collected using the Maia detector, which has an annular array of 384 silicon PIN-diode elements operated at normal incidence geometry (Ryan et al. 2018). The data for *P. xaragurensis* was obtained using a silicon drift detector (Hitachi Vortex EM-90, 80 mm<sup>2</sup>) operated in 90-degree geometry. The reason for using different detection systems is that the Maia detector was damaged and not operational at the time of the experiment for *P. xaragurensis*. In both cases, an incident energy of 12 keV was used to excite all elements of interest. The freeze-dried specimens of *P. reticulata* were held between two sheets of Ultralene thin film (4  $\mu\text{m}$ ) mounted over a frame attached to the motion stage at atmospheric temperature ( $\sim 20\text{ }^{\circ}\text{C}$ ). The fresh/hydrated samples of *P. xaragurensis* specimens were similarly mounted, and cross-sections made by hand cutting using a stainless-steel razor blade ('dry knife' method) and immediately analysed.

### Data processing of XFM data

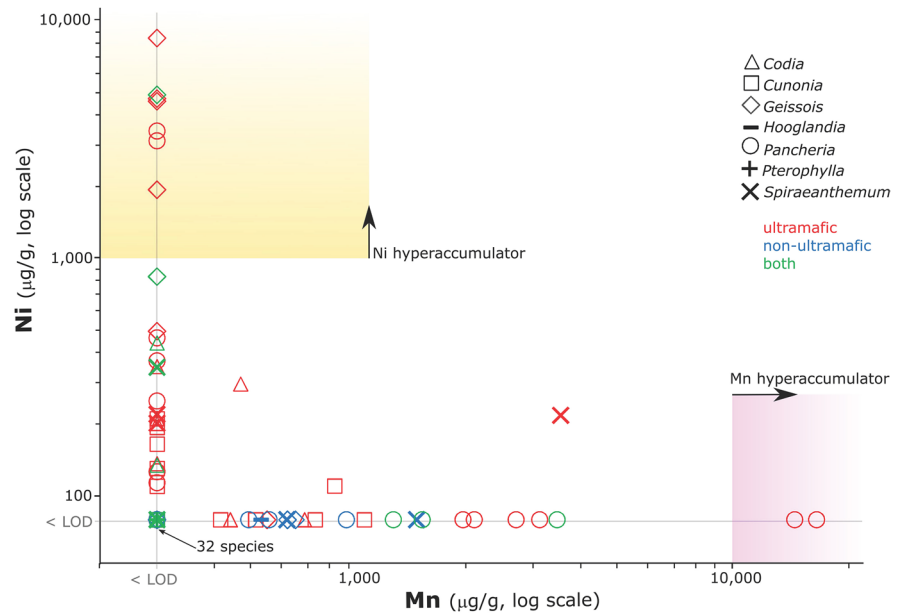
The XFM data collected with the Maia detector was analysed using GeoPIXE software (Ryan and Jamieson 1993; Ryan 2000; Ryan et al. 1990), whereas the XFM data collected with the silicon drift detector was analysed using PyMCA software (Solé et al. 2007), and exported into ImageJ as greyscale 16-bit TIFF files, and visualized using ImageJ's "Fire" lookup table (Schneider et al. 2012). The matrix file used for the spectra fitting was an assumed freeze-dried plant material composition of  $\text{C}_{31}\text{O}_{15}\text{H}_{51}\text{N}_2\text{S}_{0.8}$  with a density of  $0.75\text{ g cm}^{-3}$ , and for fresh samples the composition was  $\text{C}_{7.3}\text{O}_{33}\text{H}_{59}\text{N}_{0.7}\text{S}_{0.8}$  with a density of  $0.90\text{ g cm}^{-3}$  and considering two layers of 4  $\mu\text{m}$  Ultralene (van der Ent et al. 2019c). Note that the values reported for the fresh specimens will report per unit hydrated weight and the values for the freeze-dried specimens as dry weight.

## Results

### Incidence of nickel and manganese (hyper) accumulation in the Cunoniaceae

Handheld XRF measurements on 2519 herbarium specimens revealed overall wide ranging foliar Mn and Ni concentrations of the Cunoniaceae (Fig. 2).

**Fig. 2** Plot of Mn vs. Ni in New Caledonian Cunoniaceae. Each point represents a species, and median values were used to plot each species on a log-scale. Species substrate preferences are from Hopkins et al. (2014)



Only 32 species, from the over 91 investigated, had a median below the limit of detection for both Mn (LOD  $455 \mu\text{g g}^{-1}$ ) and Ni (LOD  $107 \mu\text{g g}^{-1}$ ), of these, 11 occur only on ultramafic soils, 15 occur on non-ultramafic soils, and six occur on both types of soils. Most of the species had relatively high concentrations of Ni or Mn, and in some cases, concentrations were very high and exceeded hyperaccumulation thresholds (Ni  $>1000 \mu\text{g g}^{-1}$ , Mn  $>10,000 \mu\text{g g}^{-1}$ ). The distribution of the median for Ni concentrations is relatively continuous (but note that the graph is plotted on a log-scale), and high Ni concentrations ( $>100 \mu\text{g g}^{-1}$ ) were only found in species growing on ultramafic soils (Fig. 2). In contrast, high Mn concentrations ( $>1000 \mu\text{g g}^{-1}$ ) were also observed on non-ultramafic soils (Fig. 2). Very few species had concomitantly high Mn and high Ni concentrations (Figs. 2 and 3), and only three species had a median for both Ni and Mn above the LOD, but none of them reached the hyperaccumulation threshold for a given element.

No species of *Hooglandia* and *Pterophylla* were detected as either Ni or Mn hyperaccumulators. In the genera *Codia* and *Cunonia* only a few species had median values close to the Ni hyperaccumulation threshold. In the genus *Spiraeanthemum*, only one species, *S. meridionale*, had Mn values close to the hyperaccumulation threshold. In the genus *Geissois*, seven species (out of 13 occurring in New Caledonia) were confirmed as Ni hyperaccumulators. In this genus only

one species (*G. belema*) occurring on ultramafic soils had Ni foliar concentrations consistently below the LOD for Ni. *Pancheria* was the only genus to contain both Ni and Mn hyperaccumulator species (Fig. 2). Two species, *P. engleriana* and *P. xaragurensis*, had high median Ni concentrations and clearly qualify as Ni hyperaccumulators (Fig. 3). Two other species, *Pancheria reticulata* and *P. multijuga*, had much higher Mn concentrations than all of the other species and qualify as Mn hyperaccumulators. The investigation will further focus on two hyperaccumulators in the genus *Pancheria*: *P. reticulata* and *P. xaragurensis*.

#### Bulk elemental concentrations in soils

Soils associated with *P. reticulata* were acidic (pH 4.50–5.24) whilst those associated with *P. xaragurensis* were slightly acidic to neutral and ranged from pH 5.77 up to pH 7.18 (Table 1). Typical for highly weathered Ferralsols, the total concentrations of Fe were extremely high (up to  $471 \text{ g kg}^{-1}$  in the soils associated with *P. xaragurensis*), while concentrations of Cr, Mn, and Ni were also high (Table 1) with total concentrations of up to  $7050 \mu\text{g g}^{-1}$  and  $16,700 \mu\text{g g}^{-1}$ ;  $7280 \mu\text{g g}^{-1}$  and  $7600 \mu\text{g g}^{-1}$ ,  $2380 \mu\text{g g}^{-1}$  and  $11,500 \mu\text{g g}^{-1}$  respectively at the localities with *P. reticulata* and *P. xaragurensis*. Other transition metals (Co and Zn) had low concentrations of  $<100 \mu\text{g g}^{-1}$  in the soils associated with *P. reticulata*; though slightly higher in the soil of

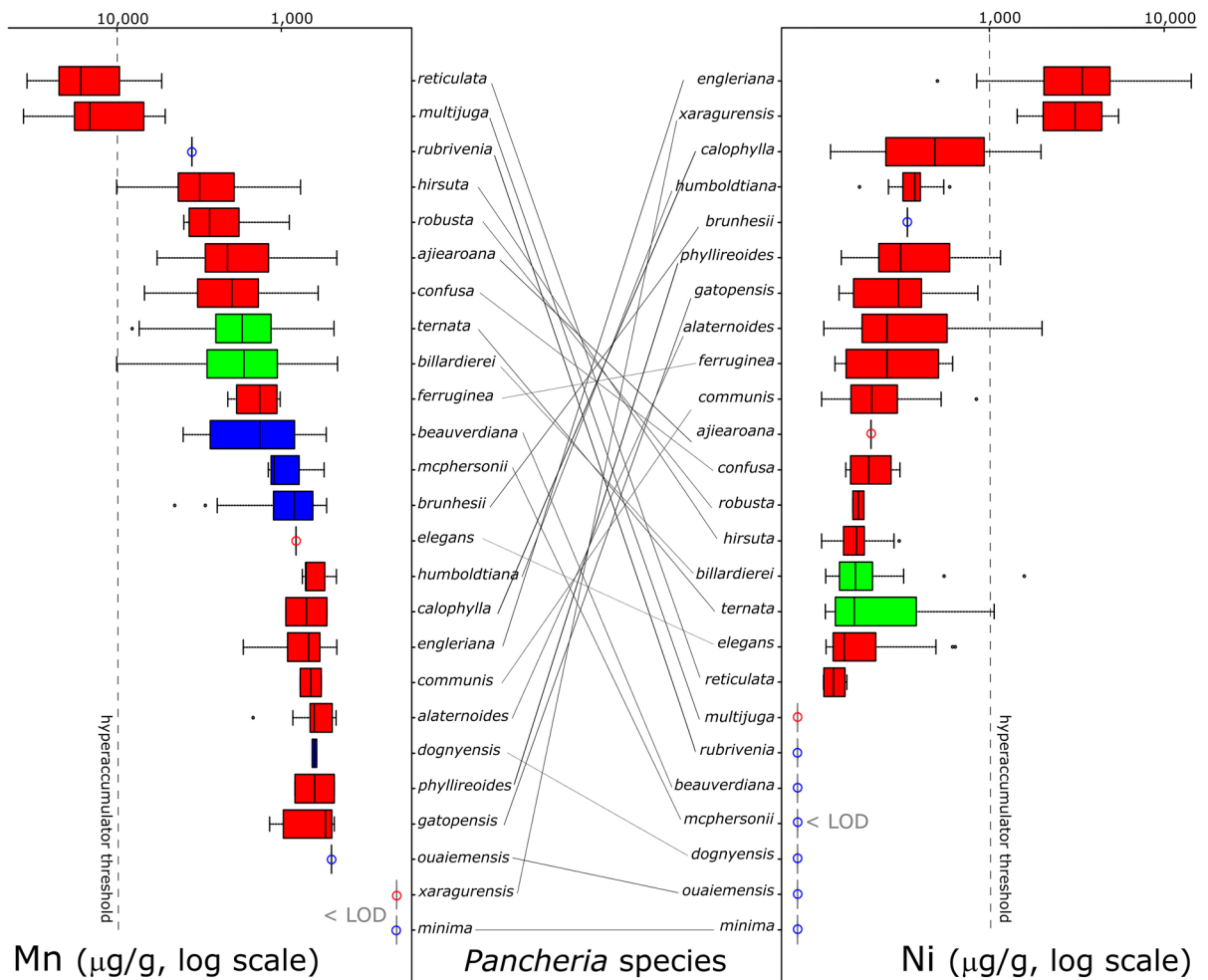


**Fig. 3** Boxplots of Mn and Ni concentrations (log-scale) of *Pancheria* species based on herbarium XRF data. Species restricted to ultramafic substrate (or almost always so) are shown in red, those restricted to non-ultramafic substrates in blue, and species occurring on both types of soils are shown in green. Values below the limit of detection (LOD) were

excluded. All measured values of Mn for *P. minima* and *P. xaragurensis*, of Mn for *P. beauverdiana*, *P. rubrivenia*, *P. multijuga*, *P. mcphersonii*, *P. dognyensis*, *P. ouaiemensis*, and *P. minima*, were below the LODs for Ni and Mn. A single value (out of 26) is above LOD for *P. brunhesii*

*P. xaragurensis* (between 300 and 1000 µg g<sup>-1</sup>). Ferralsols derived from ultramafic rocks typically have low macro-nutrient concentrations. Calcium and K had low total concentrations in the soils of both species. The phytoavailability (DTPA-extractable) of Mn was moderately high in both sites, unlike other transition elements (Co, and Zn) that had relatively low concentrations for New Caledonian ultramafic soils. Phytoavailability (DTPA-extractable) of Ni at *P. reticulata* locality was also somewhat low for New Caledonian ultramafic soils (<60 µg g<sup>-1</sup>), whilst the Ni concentration reaches

200 µg g<sup>-1</sup> (mean value 102 µg g<sup>-1</sup>) at *P. xaragurensis* site. The soil solution metal concentrations, estimated by the Sr(NO<sub>3</sub>)<sub>2</sub> extraction, were low at both sites, except for Mn which was higher at the *P. reticulata* site compared to the *P. xaragurensis* site.

**Bulk elemental concentrations in *Pancheria reticulata* and *P. xaragurensis* tissues**

The data obtained from bulk chemical analysis (Fig. 4, Suppl Table 1) generally align with the XRF

**Table 1** Soil 'extractable' elemental concentrations in the soils associated with *Pancheria reticulata* and *Pancheria xaragurensis* (values as ranges and means in  $\mu\text{g g}^{-1}$  dry weight) with Inductively Coupled Plasma Atomic Emission Spectroscopy (ICP-AES). Extraction methods are 'DTPA' (diethylenetriamine penta-acetic acid) and 'Sr(NO<sub>3</sub>)<sub>2</sub>' (0.1 M strontium nitrate)

Units	Extract	N samples	pH (H <sub>2</sub> O)	Al $\mu\text{g g}^{-1}$	Mg $\mu\text{g g}^{-1}$	K $\mu\text{g g}^{-1}$	Ca $\mu\text{g g}^{-1}$	Mn $\mu\text{g g}^{-1}$	Ni $\mu\text{g g}^{-1}$	Zn $\mu\text{g g}^{-1}$	Cr $\mu\text{g g}^{-1}$	Fe g kg <sup>-1</sup> or $\mu\text{g g}^{-1}$	Co $\mu\text{g g}^{-1}$
<i>Pancheria reticulata</i>	Total	10	(4.50–5.24)	4830 (4090–6870)	409 (285–770)	167 (82–309)	953 (579–1680)	2930 (1140–7280)	2140 (1770–2380)	80 (37–150)	3690 (2440–7050)	245(202–412)*	83 (47–132)
	DTPA	10		–	–	–	–	1080 (556–1730)	75.6 (46.3–108)	10.8 (5.61–20.3)	1.05 (0.33–4.91)	264 (146–499)	57.7 (15.0–103.3)
	Sr(NO <sub>3</sub> ) <sub>2</sub>	10		1.88 (<DL–4.45)	125 (73.9–180)	83.2 (41.2–219)	172 (20.3–456)	176 (103–266)	10.4 (4.13–19.9)	1.33 (0.38–2.66)	<DL	0.73 (0.04–5.82)	8.61 (0.46–19.2)
<i>Pancheria xaragurensis</i>	Total	5	(5.77–7.18)										
	DTPA	5						428 (163–742)	102 (9.5–204)	1.28 (0.88–2.07)	0.22 (0.09–0.31)	42.9 (20.0–97.6)	62.1 (25.9–88.9)
	Sr(NO <sub>3</sub> ) <sub>2</sub>	5		0.07 (0.06–0.1)	282 (26.1–530)	11.5 (9.50–13.6)	69.4 (32.2–116.3)	6.29 (2–14.3)	1.2 (0.2–2.6)	0.01 (<DL–0.02)	0.05 (0.03–0.06)	3.2 (2.70–4.1)	0.14 (0.02–0.42)



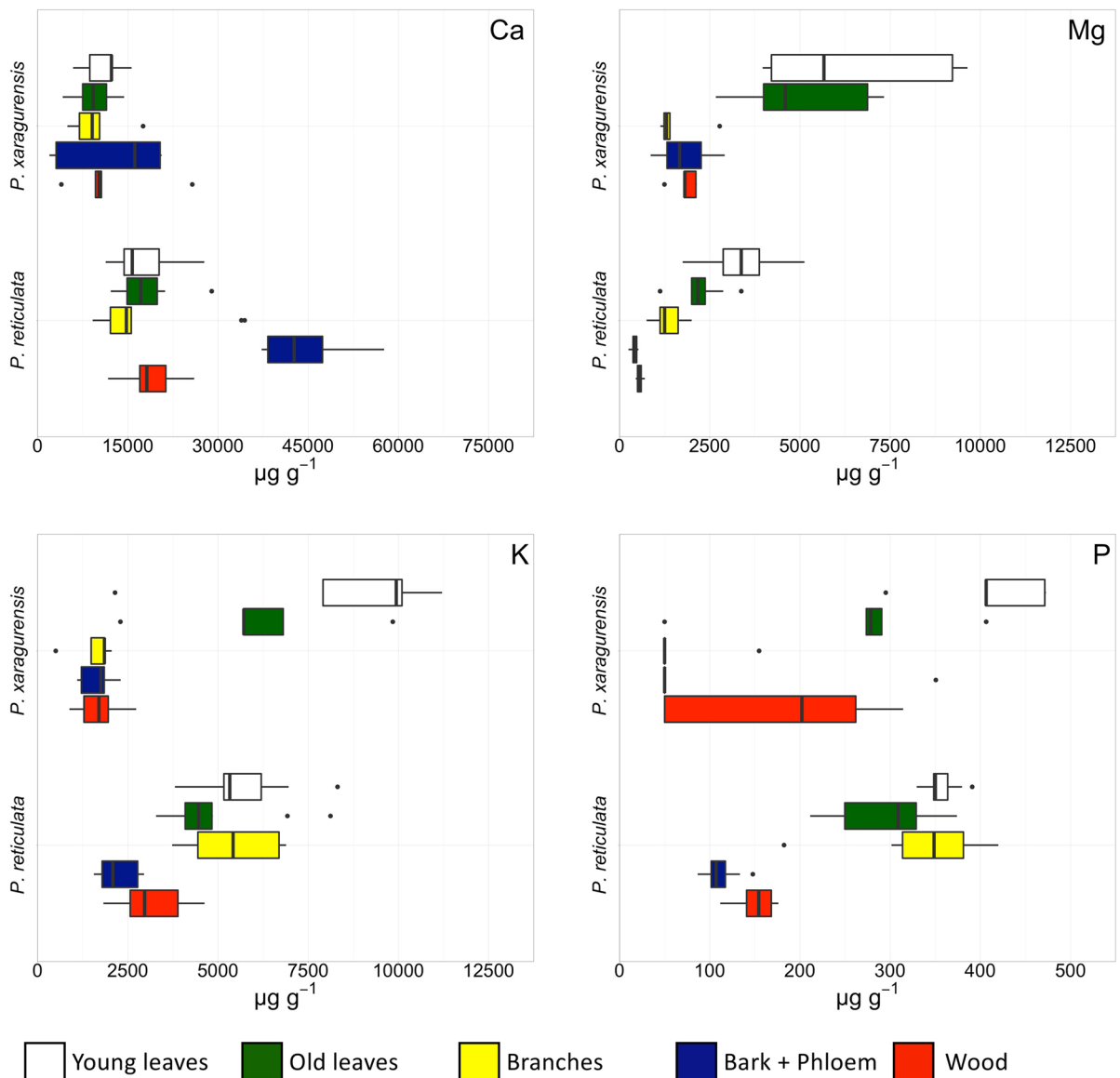


**Fig. 4** Boxplots of elemental concentrations (Ca, Mg, K, P) obtained with Inductively Coupled Plasma Atomic Emission Spectroscopy (ICP-AES) analysis of different plant parts of *Pancheria reticulata* and *P. xaragurensis*

assessment of herbarium specimens of *Pancheria reticulata* (Mn XRF values ranging  $5300\text{--}35,200 \mu\text{g g}^{-1}$ ) and *Pancheria xaragurensis* (Ni XRF values ranging  $1440\text{--}5490 \mu\text{g g}^{-1}$ ) confirming the hyperaccumulator status of these species. (Fig. 3). In both species, the concentrations greatly vary between the plants, even though they were collected from the same site. *Pancheria reticulata* had particularly high foliar Mn concentrations, consistently above the hyperaccumulation threshold ( $19,500\text{--}57,800 \mu\text{g g}^{-1}$ ). The young and

old leaves of *P. reticulata* similarly had very high mean Mn concentrations (mean value of  $\sim 31,000 \mu\text{g g}^{-1}$ ) (Fig. 4). The branches were also strongly enriched in Mn with a mean of  $19,200 \mu\text{g g}^{-1}$ , due to high Mn enrichment in both the wood and bark (including the phloem). In *P. xaragurensis* Ni concentrations were higher in old leaves, but much lower in branches (Fig. 4). The concentrations of the other trace elements Co, Fe, and Zn were uniformly low in all of the plant tissues (mean  $< 100 \mu\text{g g}^{-1}$  for Co and Zn).

In both species, the concentrations of the elements Ca, K, P, Mg (Fig. 5) were comparable between the old and young leaves, whilst P and K concentrations in the leaves were similar in both species.

#### Elemental localization in *Pancheria reticulata*

The elemental maps obtained from the synchrotron-based XFM analysis were visually interpreted for localization of elemental distribution and prevailing

relative concentrations estimated based on comparisons of the quantitative concentration scale and anatomical features in the maps. The data from the leaf cross-sections show that Mn had particularly high concentrations ( $30\text{--}40\text{ g kg}^{-1}$ ) in the large cells of the adaxial hypodermis and in lower concentrations in the abaxial epidermal cells, apoplastic space of the collenchyma, and more diffusely occurring in the mesophyll (Figs. 6 and 7). The localizations of K and Mn are very similar, yet with a distinct

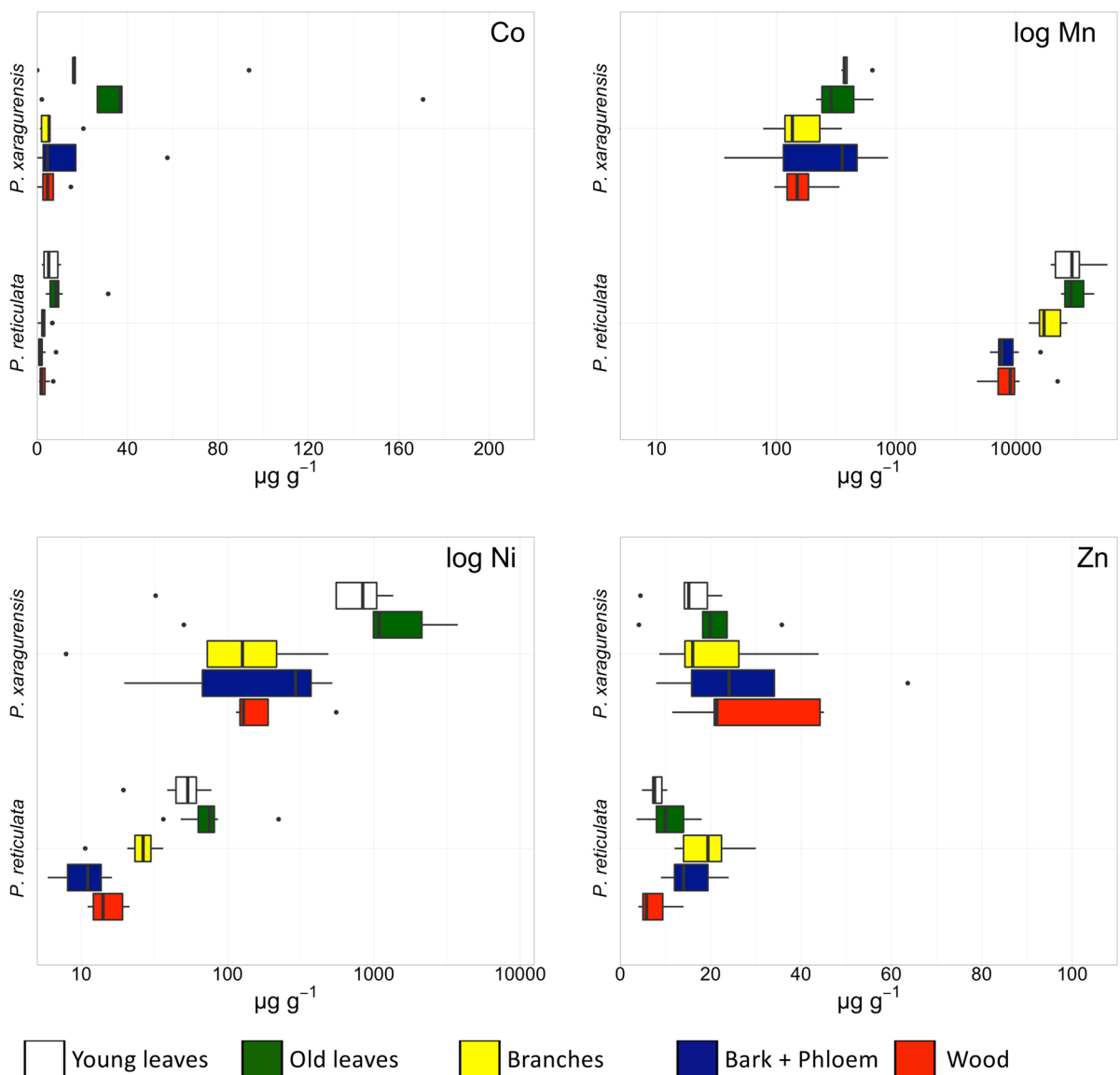
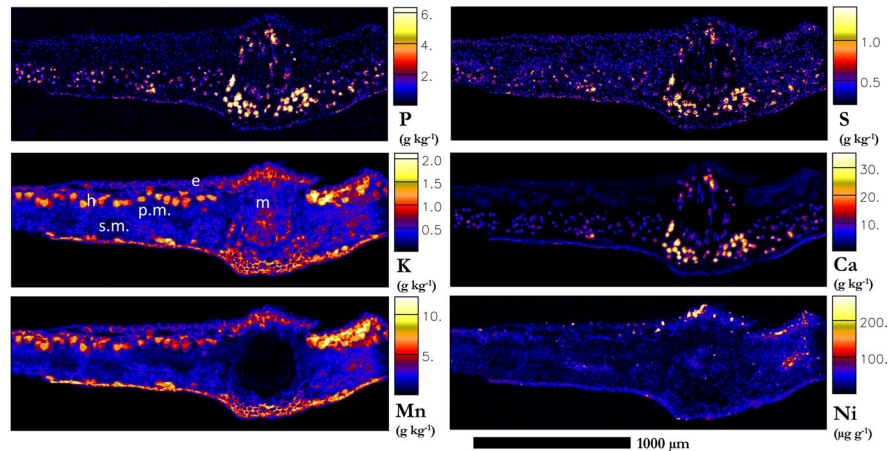


**Fig. 5** Boxplots of elemental concentrations (Co, Mn, Ni, Zn) obtained with Inductively Coupled Plasma Atomic Emission Spectroscopy (ICP-AES) analysis of different plant parts of *Pancheria reticulata* and *P. xaragurensis*

**Fig. 6** Synchrotron-based XFM maps of P, S, K, Ca, Mn, Ni of a freeze-dried cross-section of a *Pancheria reticulata* leaf at the midrib with part of the lamina. Abbreviations of anatomical features indicated: e, epidermis; h, hypodermal cells; s.m., spongy mesophyll; p.m., palisade mesophyll; m. midrib



difference in the midrib xylem where there is hardly any prevailing Mn, whilst K concentrations are high ( $\sim 10 \text{ g kg}^{-1}$ ) (Fig. 6). Overall Ni is relatively low in the leaves, it is present in the upper epidermis, but in negligible quantities (max  $\sim 200 \mu\text{g g}^{-1}$ ) (Fig. 6). Phosphorous, S, and Ca ( $50\text{--}100 \text{ g kg}^{-1}$ ) are concentrated in the collenchyma and the spongy mesophyll (Fig. 6). The upper epidermis and palisade mesophyll appear to have very low prevailing concentrations of P and Ca, whilst spots of  $<10 \text{ g kg}^{-1}$  S are homogeneously scattered there. The portion of the freeze-dried leaf lamina cross-sections (Figs. 7 and 8) originate from different portions of the same sample at different dimensions, resolutions, and dwell time. These elemental maps confirm the distributions and concentrations of P, K, Ca, and Mn as presented in Fig. 5. Phosphorus, S and Ca are co-localized while K and Mn are co-localized albeit in different concentration ratios (Fig. 8). There is a notable enrichment of P and Ca in the spongy mesophyll, with the Ca concentrations being four-fold that of P. High concentrations of K ( $\geq 15 \text{ g kg}^{-1}$ ) and Mn ( $\geq 100 \text{ g kg}^{-1}$ ) were measured for the adaxial hypodermis cells, with highest

concentrations within the cells. The abaxial epidermal cells are of much smaller size with however a notable concentration of K ( $15 \text{ g kg}^{-1}$ ) and Mn (up to  $100 \text{ g kg}^{-1}$ ) (Fig. 7). A high-resolution scan ( $5 \mu\text{m}$ ) of the adaxial epidermis and palisade mesophyll was obtained (Fig. 8), which reveals co-localization of K and Mn in large sub-epidermal cells and in the apoplastic space. Excess foliar Mn is, however, likely confined to what appear to be large vacuoles in the centre of these cells, that were strongly enriched (Mn exceeding  $100 \text{ g kg}^{-1}$ ) and is less notable in the apoplastic space.

#### Elemental localization in *Pancheria xaragurensis*

Synchrotron-based XFM analysis of leaf cross sections show that Ni was highly enriched in a broad zone encompassing the abaxial and adaxial epidermal cells as in the collenchyma of the midrib (Fig. 9) and in several locations crossing into the mesophyll (Fig. 10). The distributions of K and Ni are very similar, but in contrast, Ca is present mainly as deposits (likely Ca-oxalate) lining the mesophyll and the

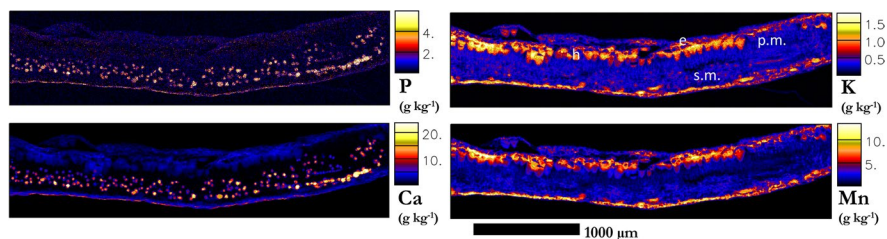
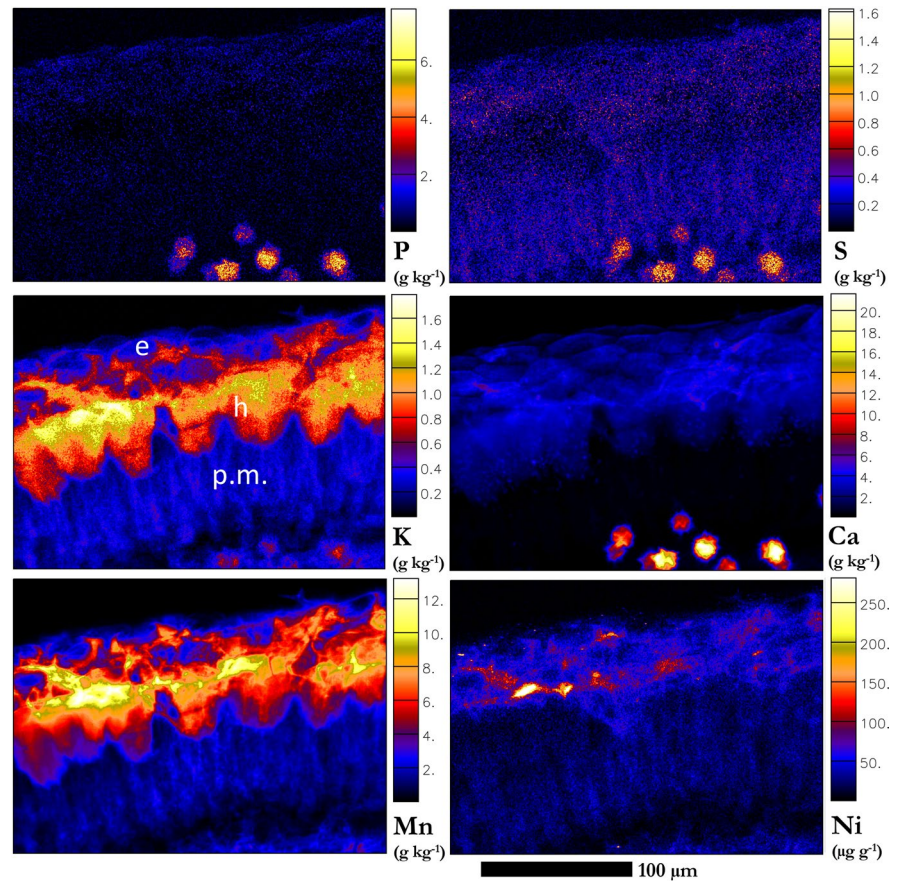


**Fig. 7** Synchrotron-based XFM maps of P, S, K, Ca, Mn, Ni of a freeze-dried cross-section of a *Pancheria reticulata* leaf blade. Abbreviations of anatomical features indicated: e, epidermis; h, hypodermal cells; s.m., spongy mesophyll; p.m., palisade mesophyll

**Fig. 8** Synchrotron-based XFM maps of K, Ca, Mn, Ni of a freeze-dried *Pancheria reticulata* cross-section of the leaf. Magnification on upper epidermis and palisade tissues. Abbreviations of anatomical features indicated: e, epidermis; h, hypodermal cells; p.m., palisade mesophyll



sclerenchyma at the periphery of the midvein vascular bundle (Fig. 9). Higher-resolution details scans of the leaf lamina (Fig. 10) reveal that Ni is extremely enriched in the epidermis, mainly in the adaxial side of the lamina. Notable Ni enrichment across the leaf lamina occurs in the leaf sheath surrounding the vascular bundle (Fig. 10). Although more evenly distributed throughout the leaf lamina, Ca enrichment also occurs in the vascular bundles.

## Discussion

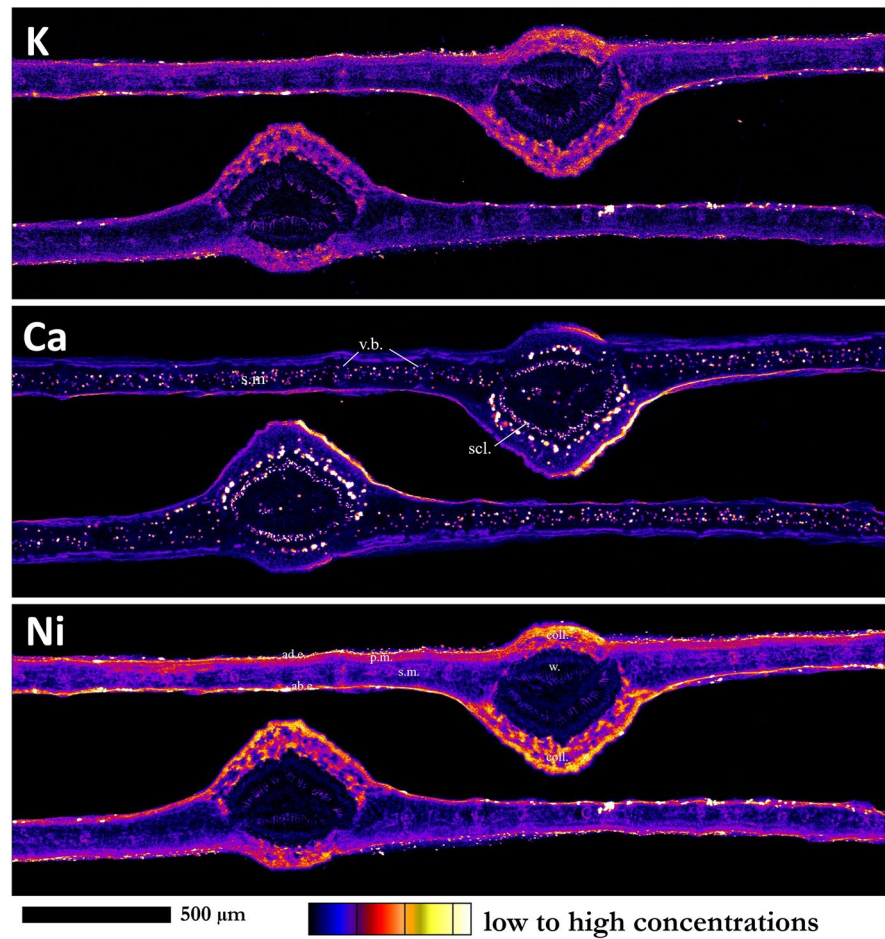
### Nickel and manganese hyperaccumulation in Cunoniaceae

As expected, high foliar Ni concentrations are restricted in New Caledonian Cunoniaceae to the species occurring on ultramafic soils, where this element is enriched (Latham et al. 1978). However, although the highest foliar Mn values are observed in plants from

ultramafic soils, Mn concentrations within the toxic range for most plants (Krämer 2010) are also observed in plants growing on non-ultramafic soils. Species may have high foliar Ni concentrations or high foliar Mn concentrations, but not high concentrations of both elements concomitantly. These different adaptations observed on ultramafic soils may be indicative of a trade-off between the uptake/transport and/or storing of these two elements in plants. Although the differences could also be associated to different local soil conditions for each species, we believe this to be unlikely. *Pancheria reticulata* (Mn hyperaccumulator), *P. engleriana* (Ni hyperaccumulator) and *P. calophylla* (with moderate Mn and Ni accumulation) can be observed in sympatry on Mount Paéoua (Y. Pillon pers. obs.). It is more probable that these species have different physiological adaptations to cope with harsh conditions which explains their differences in metal concentrations in sympatry (Pillon et al. 2019b). This is in line with the major physiological diversity associated with New Caledonian plant radiation (Pillon



**Fig. 9** Synchrotron-based XFM maps of K, Ca, Ni of fresh hydrated cross-sections of *Pancheria xaragurensis* leaf midribs and lamina. Abbreviations of anatomical features indicated: ad.e, adaxial epidermis; ab.e, abaxial epidermis; coll., collenchyma; scl., sclerenchyma; s.m., spongy mesophyll; p.m., palisade mesophyll; v.b., vascular bundles; w., wood



et al. 2014), and nutrient limitation adaptations seen on infertile soils (Hopper 2009; Pillon et al. 2021b).

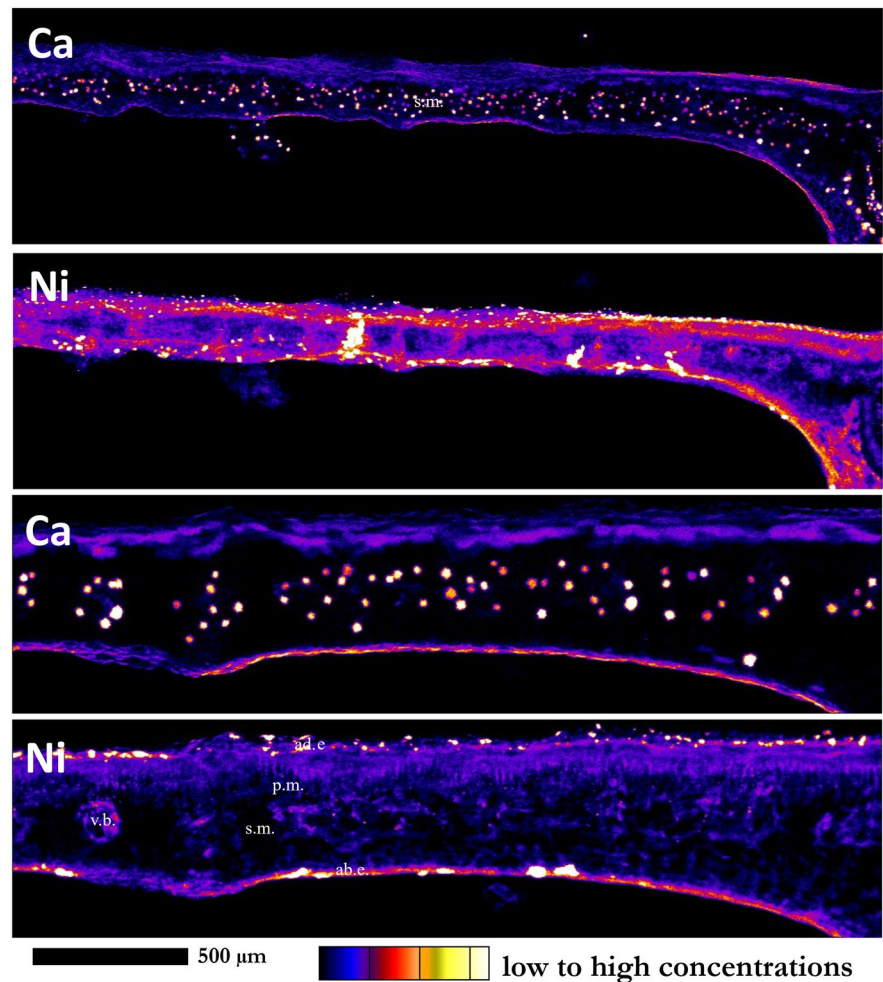
Outside of New Caledonia, high foliar Mn concentrations have also been reported in Cunoniaceae from South America (genus *Weinmannia*), although not reaching the hyperaccumulation threshold (Belloeil et al. 2021). Cunoniaceae also generally tend to be over-represented on ultramafic soils (Pillon et al. 2019a). The fact that adaptation to ultramafic soils and metal (hyper)accumulation are observed in multiple and distantly related genera, and in different regions, indicates that the Cunoniaceae could have an ancestral ability to cope with challenging edaphic conditions and to uptake and store metals in their tissues. The Cunoniaceae belong to the Oxalidales order that includes five other small to medium size families. Nickel hyperaccumulation has also been reported in two of these families on ultramafic substrates: the Indonesian *Sarcotheca celebica* (Oxalidaceae,

Galey et al. 2017) and the Cuban *Rourea glabra* (Connaraceae, Belloeil et al. 2021). Therefore, the greater capacity to adapt to ultramafic soils and to become a metal hyperaccumulator may be ancestral to the entire Oxalidales order.

Most genera with hyperaccumulators are specialised for a single element (e.g., Ni in *Hybanthus*, *Pycnanandra*). The number of genera where hyperaccumulation of multiple elements is observed is still limited and includes *Noccaea* (Ni, Zn, Cd) and *Arabidopsis* (Zn, Cd) in the Brassicaceae (Brassicales), *Dichapetalum* (Ni, Zn) in the Dichapetalaceae (Malpighiaceae), and *Phyllanthus* including *Glochidion* (Ni, Co, Mn) (Nkrumah et al. 2018; van der Ent et al. 2018a) in the Phyllanthaceae (Malpighiales). In the Cunoniaceae (Oxalidales), Ni and Al hyperaccumulation have previously been reported within the recently diversified New Caledonian genus *Geissois* (Pillon et al. 2014). *Pancheria* is thus a novel example



**Fig. 10** Synchrotron-based XFM maps of Ca, Mn, Ni of fresh hydrated cross-sections of *Pancheria xaragurensis* lamina. Abbreviations of anatomical features indicated: ad.e., adaxial epidermis; ab.e., abaxial epidermis; m., spongy mesophyll; p.m., palisade mesophyll; v.b., vascular bundles



of a genus where hyperaccumulation of multiple elements is observed. *Pancheria* diverged from its sister group, *Cunonia*, 26.9 million years ago (Pillon et al. 2021a), with a very similar level of morphological and species diversity in New Caledonia, an equivalent preference for ultramafic substrates, but which has much lower affinities for metals. Data obtained from analyses of leaves by ICP-AES and by herbarium XRF on *Pancheria reticulata* confirmed that this species has extremely high Mn concentration in its leaves ( $19.5\text{--}57.7\text{ g kg}^{-1}$ ,  $n=20$ ). To our knowledge this is the highest Mn concentration in leaves ever found in a hyperaccumulator species so far, with *Vivotia neurophylla* (Proteaceae) from New Caledonia spanning a similar concentration range ( $15.8\text{--}55.2\text{ g kg}^{-1}$ ,  $n=20$ ) (Jaffré 1979). *Pancheria multijuga*, another Mn hyperaccumulator detected by herbarium XRF analysis, also had extremely high leaf

Mn concentrations ( $25.7\text{--}29.9\text{ g kg}^{-1}$ ,  $n=2$ ), confirmed by ICP-AES analysis (Suppl Table 2).

#### Influence of soil chemistry

Tropical Ni hyperaccumulation has always been reported from ultramafic soils with high Ni concentrations (van der Ent et al. 2016, 2017b; Echevarria 2021), whilst Mn hyperaccumulation has been reported from a diverse array of types soils. Several plant species occurring on soils with low concentrations of exchangeable Mn availability have been found to accumulate foliar Mn to much higher concentrations than in most other plants (Marschner 2002; Memon et al. 1979; Foulds 2003). The differences in Mn accumulation can also be explained to differences in Mn solubilization in the rooting zone (Lambers et al. 2015). Higher foliar Mn is often seen in plants

that release large amounts of carboxylates from their roots that strongly acidify the rhizosphere (Lambers et al. 2010). In the Proteaceae for instance, Mn accumulation is due to the release of carboxylates by specialized cluster roots (Lambers et al. 2015). As such, in New Caledonia, Jaffré (1979) found that the among species growing on ferralitic soils with low exchange capacity, Proteaceae generally accumulated more Mn than co-occurring species belonging to different families. Cluster roots are, however, not known in the Cunoniaceae. Previous studies did report on arbuscular mycorrhiza associations in some Cunoniaceae from New Caledonia growing on metal-rich Ferral-sols (Perrier et al. 2006), and microbial activity could increase the mobility of metal (Amir and Pineau 2003a, b; Berthelin et al. 1995). Further studies should investigate the correlation between microbial activity and Ni/Mn hyperaccumulation in the Cunoniaceae.

Manganese hyperaccumulation was shown to vary between the different maquis and soil properties, with acidic colluvial and gravelly ferralitic soils being the most propitious for strong hyperaccumulation (Jaffré 1980). In line with this finding, *P. reticulata* at Mont Mou grows on acidic gravelly ferralitic soils. Manganese bioavailability depends on soil pH and is largely independent from total or exchangeable soil Mn concentrations (Fernando et al. 2008b; Jaffré 1980). As such, Fernando et al. (2008b) found that two subspecies of *Denhamia founieri* (previously *Maytenus founieri*) strongly differ in their foliar Mn concentrations mainly in response to soil pH, in spite of lower Mn soil concentrations for the highest hyperaccumulation sites. In our study, we found similar phytoavailability of Mn in the soils associated with both species, but the soil pH at *P. reticulata* site was also strongly acidic (pH 4.50–5.24). At the *P. xaragurensis* site, the soil pH was, however, slightly acidic to neutral, which are natural conditions that favour Ni hyperaccumulation (Kukier et al. 2004). Metal mobilisation in the rhizosphere is undoubtedly a major factor associated with metal hyperaccumulation for Mn and would explain why there is not strict relationship between foliar metal accumulation and concentrations in the soil.

#### Distribution of Mn and Ni within the plants

We found relatively high Mn concentrations in the bark (cortex and phloem), as previously found for other Mn hyperaccumulators (Bidwell et al. 2002;

Fernando et al. 2006), but also in the wood of *P. reticulata*, with variation that could at least partially be explained by the remaining sap contained in the wood samples. Investigations by Fernando et al. (2012) using cryogenic Scanning Electron Microscopy with Energy-Dispersive Spectroscopy (SEM-EDS) obtained in vivo quantitative elemental composition from frozen-hydrated cells. These detailed investigations of leaves have demonstrated that Mn foliar concentration pattern differed markedly between species, a trait that appears to be specific to Mn hyperaccumulation (Fernando et al. 2008a). The highest localized Mn concentrations have been found in low/non-photosynthetic cells types, such as the epidermal cells, including the trichomes and leaf hairs, multiseriate hypodermal cells (e.g. *Denhamia founieri*) or spongy mesophyll cells (e.g. *Garcinia amplexicaulis*) (Fernando et al. 2006, 2012). In addition, and in contrast to the foliar localization of other hyperaccumulated metals, high Mn concentrations also occur in the multi-layered highly vacuolated large palisade mesophyll cells (Fernando et al. 2006, 2012).

The localization pattern of Mn in *P. reticulata* leaves revealed that the highest localized concentrations are in non-photosynthetic tissues, i.e., principally in large hypodermal cells, and in the apoplastic space in the collenchyma. The primary Mn deposit site in the large epidermal cell, was also found in *Grevillea exul* s.l. and *G. meisneri*, although their Mn bulk concentrations (3000–4000  $\mu\text{g g}^{-1}$ ) did not necessarily attain the hyperaccumulation threshold values (Fernando et al. 2006, 2008a; Bihanic et al. 2021). In contrast to *Viotia neurophylla*, Mn was not detected at high concentrations in the palisade (photosynthetic) tissues. Altogether these results suggest that the Mn concentration sites are not related to the level of accumulation and that leaf anatomy (particularly cell-size) is an important driver of sequestration, and potentially an important evolutionary prerequisite in the evolution of Mn hyperaccumulation. The cell size was previously noted to influence the preferential accumulation site in Mn hyperaccumulators (Fernando et al. 2012). This finds support by the fact that most Mn hyperaccumulator plants are often sclerophyllous species with a xerophytic leaf anatomy (multiple layers of epidermal cells or palisades tissues, hypodermal tissues). The abundant sclerophyllous vegetation in New Caledonian maquis could explain the diversity of Mn hyperaccumulators found

in New Caledonia, although not all sclerophyll species are hyperaccumulators of course.

The localization of Ni in *P. xaragurensis* is different to Mn in *P. reticulata*. It also differs from the majority of Ni hyperaccumulator plants studied to date in which Ni is universally localized in the vacuoles of the epidermal cells (Bidwell et al. 2004; Kachenko et al. 2008; Küpper et al. 2001; Mesjasz-Przybyłowicz et al. 2016; van der Ent et al. 2017a, 2018b; Broadhurst et al. 2004). The patterns of Ni enrichment in *P. xaragurensis* are akin to extracellular detoxification mechanisms in which Ni is expelled from the apoplast and forms Ni-rich deposits. In the case of *P. xaragurensis*, the process possibly starts by Ni-loading into vacuoles of epidermal cells which leads to cell death and eventually the formation of Ni-rich plaques. Similar observations have been made in the Co-Ni hyperaccumulator *Glochidion cf. sericeum* from Borneo in which Co is excreted in the form of lesions in the epidermal region of the leaf lamina (van der Ent et al. 2018a). Curiously, this type of ecophysiological response is typically associated with Mn toxicity in crop plants in which characteristic ‘lesions’ form in which Mn is dumped, often near trichomes bases (Blamey et al. 1986). Hence, it appears that adaptations of *P. xaragurensis* to sequester and tolerate excess Ni on the tissue/cellular scale is distinct from the mechanisms responsible for Mn tolerance in *P. reticulata*. We also found high Ni concentrations in the parenchymatous bundle sheath surrounding the vascular bundle. This elemental distribution pattern was not found in the Mn hyperaccumulator *P. reticulata*. Vein sheathing in *Pancheria* was found to be of systematic significance, as species strongly differ in their sheathing features (Rao and Dickison 1985). Bundle-sheath extensions connect the sheath of the larger vein with both epidermal layers (Evert 2006). Further studies should investigate the role of parenchymatous bundle sheaths in Ni hyperaccumulation, and more specifically the translocation of Ni from the vascular system to the epidermal cells.

## Conclusions

The Cunoniaceae of New Caledonia have a strong affinity with metals and high foliar Ni and high Mn concentrations are observed in many species, including several clear examples of hyperaccumulation.

There appears to be a trade-off between foliar Ni and Mn concentrations with species either hyperaccumulating one of the other. Nickel and Al hyperaccumulation had previously been reported in *Geissois* (Pillon et al. 2014) and this study revealed that the second largest endemic genus of New Caledonia, *Pancheria*, also displays a remarkable physiological diversity with Ni hyperaccumulators and Mn hyperaccumulators. The detailed study of *P. reticulata* (Mn hyperaccumulator), and *P. xaragurensis* (Ni hyperaccumulator) revealed that localization of Mn and Ni at the tissue (and organ) level differs between the two species. Manganese and Ni accumulation are two different adaptations observed on ultramafic substrates that do not appear to be explained by contrasting soils conditions or to be a simple competition between the two metals that may transit through the same membrane transporters, but instead rely on distinct physiological pathways. Such contrasting adaptations can appear over relatively short evolutionary time. This diversity of physiological coping mechanisms on substrate with low fertility (ultramafic) is in line with the hypothesis formulated by Hopper (2009) on Old Climatically-Buffered Infertile Landscapes, that likely extends to New Caledonia (Pillon et al. 2021b).

**Acknowledgements** This research was undertaken at P06 at DESY, a member of the Helmholtz Association (HGF). V. Gei was the recipient of an Australia Awards PhD Scholarship from the Australian Federal Government. The authors thank the Province Sud de Nouvelle-Calédonie for permission to collect the plant material samples (N° 4508-2018/ARR/DENV). The authors thank Vanessa Hequet for collecting *P. multijuga* at Mont Humboldt.

**Author contributions** VG, AvdE, SI, BF and PDE conducted the fieldwork and collected the samples. VG, AvdE, SI, BF, EMP, GE, KMS and PDE conducted the synchrotron XFM experiment. KMS performed the XFM data processing and analysis. VG and AvdE performed the histochemical and anatomical studies. VG conducted and bulk elemental analysis. VG, AvdE, SI, BF, EMP, GE, KMS, YP and PDE wrote the manuscript.

**Funding** Open Access funding enabled and organized by CAUL and its Member Institutions The research leading to this result has been supported by the project CALIPSOplus under the Grant Agreement 730872 from the EU Framework Programme for Research and Innovation HORIZON 2020. A. van der Ent was the recipient of a Discovery Early Career Researcher Award (DE160100429) from the Australian Research Council. Part of this work was funded by a Pacific Fund Project led by S. Isnard (2020–2022).

**Data availability** The data generated during the current study are available as Supplementary Information

## Declarations

**Competing interests** The authors declare no conflicts of interest relevant to the content of this article.

**Open Access** This article is licensed under a Creative Commons Attribution 4.0 International License, which permits use, sharing, adaptation, distribution and reproduction in any medium or format, as long as you give appropriate credit to the original author(s) and the source, provide a link to the Creative Commons licence, and indicate if changes were made. The images or other third party material in this article are included in the article's Creative Commons licence, unless indicated otherwise in a credit line to the material. If material is not included in the article's Creative Commons licence and your intended use is not permitted by statutory regulation or exceeds the permitted use, you will need to obtain permission directly from the copyright holder. To view a copy of this licence, visit <http://creativecommons.org/licenses/by/4.0/>.

## References

- Amir H, Pineau R (2003a) Relationship between extractable Ni, Co and other metals and some microbiological characteristics of different ultramafic soils from New Caledonia. *Aust J Soil Res* 41:215–228
- Amir H, Pineau R (2003b) Release of Ni and Co by microbial activity in new Caledonian ultramafic soils. *Can J Microbiol* 49:288–293. <https://doi.org/10.1139/w03-039>
- Baker AJM (1981) Accumulators and excluders—strategies in the response of plants to heavy metals. *J Plant Nutr* 3:643–654. <https://doi.org/10.1080/01904168109362867>
- Baker AJM, Brooks RR (1989) Terrestrial higher plants which hyperaccumulate metallic elements - a review of their distribution, ecology and phytochemistry. *Biorecovery* 1:81–126. <https://doi.org/10.1080/01904168109362867>
- Belloeil C, Jouannais P, Malfaisan C, Reyes Fernández R, Lopez S, Navarrete Gutierrez DM, Maeder-Pras S, Villanueva P, Tisserand R, Gallopin M, Alfonso-Gonzalez D, Fuentes Marrero IM, Muller S, Invernon V, Pillon Y, Echevarria G, Berazaín Iturralde R, Merlot S (2021) The X-ray fluorescence screening of multiple elements in herbarium specimens from the Neotropical region reveals new records of metal accumulation in plants. *Metallomics* 13:mfab045. <https://doi.org/10.1093/mtomcs/mfab045>
- Berthelin J, Munier-Lamy C, Leyval C (1995) Effect of microorganisms on mobility of heavy metals in soils. In: Huang PM (ed) *Environmental impact of soil component interactions*, 2nd edn. CRC Press, Boca Raton, pp 3–17
- Bidwell SD, Woodrow IE, Batianoff GN, Sommer-Knudsen J (2002) Hyperaccumulation of manganese in the rainforest tree *Austrorhynchus bidwillii* (Myrtaceae) from Queensland, Australia. *Funct Plant Biol* 29:899–905. <https://doi.org/10.1071/PP01192>
- Bidwell SD, Crawford SA, Woodrow IE, Sommer-Knudsen J, Marshall AT (2004) Sub-cellular localization of Ni in the hyperaccumulator, *Hybanthus floribundus* (Lindley) F. Muell. *Plant Cell Environ* 27:705–716
- Bihanic C, Petit E, Perrot R, Cases L, Garcia A, Pelissier F, Poullain C, Rivard C, Hossaert-McKey M, McKey D, Grison C (2021) Manganese distribution in the Mn-hyperaccumulator *Grevillea meisneri* from New Caledonia. *Sci Rep* 11:23780. <https://doi.org/10.1038/s41598-021-03151-9>
- Blamey FPC, Edwards DG, Asher CJ (1986) Role of trichomes in sunflower tolerance to manganese toxicity. *Plant Soil* 91:171–180
- Bradford JC, Hopkins HC, Barnes RW (2004) Cunoniaceae. In: Kubitzki K (ed) *Flowering plants Dicotyledons the families and genera of vascular plants*, 6th edn. Springer, Berlin, Heidelberg, pp 91–111
- Broadhurst C, Chaney RL, Angle J, Erbe E, Maugeul T (2004) Nickel localization and response to increasing Ni soil levels in leaves of the Ni hyperaccumulator *Alyssum murale*. *Plant Soil* 265:225–242
- Echevarria G (2021) Genesis and behaviour of ultramafic soils and consequences for nickel biogeochemistry. In: van der Ent A, Baker AJM, Echevarria G, Simonnot M-O, Morel JL (eds) *Agromining: farming for metals: extracting unconventional resources using plants*. Springer International Publishing, Cham, pp 215–238
- Evert RF (2006) *Esau's Plant Anatomy*. A John Wiley & Sons, Inc., Hoboken
- Fernando DR, Batianoff GN, Baker AJ, Woodrow IE (2006) In vivo localization of manganese in the hyperaccumulator *Gossia bidwillii* (Benth.) N. Snow & Guymer (Myrtaceae) by cryo-SEM/EDAX. *Plant Cell Environ* 29:1012–1020. <https://doi.org/10.1111/j.1365-3040.2006.01498.x>
- Fernando DR, Woodrow IE, Bakkaus EJ, Collins RN, Baker AJM, Batianoff GN (2007) Variability of Mn hyperaccumulation in the Australian rainforest tree *Gossia bidwillii* (Myrtaceae). *Plant Soil* 29:145–152
- Fernando DR, Marshall AT, Gouget B, Carrière M, Collins RN, Woodrow IE, Baker AJ (2008a) Novel pattern of foliar metal distribution in a manganese hyperaccumulator. *Funct Plant Biol* 35:193–200. <https://doi.org/10.1071/FP07272>
- Fernando DR, Woodrow IE, Jaffré T, Dumontet V, Marshall AT, Baker AJM (2008b) Foliar manganese accumulation by *Maytenus founieri* (Celastraceae) in its native new Caledonian habitats: populational variation and localization by X-ray microanalysis. *New Phytol* 177:178–185. <https://doi.org/10.1111/j.1469-8137.2007.02253.x>
- Fernando DR, Guymer G, Reeves RD, Woodrow IE, Baker AJ, Batianoff GN (2009) Foliar Mn accumulation in eastern Australian herbarium specimens: prospecting for 'new' Mn hyperaccumulators and potential applications in taxonomy. *Ann Bot* 103:931–939. <https://doi.org/10.1093/aob/mcp013>
- Fernando DR, Woodrow IE, Baker AJ, Marshall AT (2012) Plant homeostasis of foliar manganese sinks: specific variation in hyperaccumulators. *Planta* 236:1459–1470. <https://doi.org/10.1007/s00425-012-1699-6>



- Fernando DR, Marshall A, Baker AJM, Mizuno T (2013) Microbeam methodologies as powerful tools in manganese hyperaccumulation research: present status and future directions. *Front Plant Sci* 4:319. <https://doi.org/10.3389/fpls.2013.00319>
- Foulds W (2003) Nutrient concentrations of foliage and soil in South-Western Australia. *New Phytol* 125:529–546
- Galey ML, van der Ent A, Iqbal MCM, Rajakaruna N (2017) Ultramafic geocology of south and Southeast Asia. *Bot Stud* 58:18. <https://doi.org/10.1186/s40529-017-0167-9>
- Gei V, Echevarria G, Erskine PD, Isnard S, Fogliani B, Montargès-Pelletier E, Jaffré T, Spiers KM, Garvoet J, van der Ent A (2020a) Soil chemistry, elemental profiles and elemental distribution in nickel hyperaccumulator species from New Caledonia. *Plant Soil* 457:293–320. <https://doi.org/10.1007/s11104-020-04714-x>
- Gei V, Isnard S, Erskine P, Echevarria G, Fogliani B, Jaffré T, van der Ent A (2020b) A systematic assessment of the occurrence of trace element hyperaccumulation in the flora of New Caledonia. *Bot J Linn Soc* 194:1–22
- Hopkins HCF, Pillon Y (2011) Further new endemic taxa of Cunoniaceae from New Caledonia. *Kew Bull* 66:405–423
- Hopkins HC, Pillon Y, Hoogland RD (2014) Cunoniaceae: flore de la Nouvelle-Calédonie. Muséum national d'Histoire naturelle/IRD, Paris
- Hopper SD (2009) OCBIL theory: towards an integrated understanding of the evolution, ecology and conservation of biodiversity on old, climatically buffered, infertile landscapes. *Plant Soil* 322:49–86. <https://doi.org/10.1007/s11104-009-0068-0>
- Isnard S, L'Huillier L, Rigault F, Jaffré T (2016) How did the ultramafic soils shape the flora of the new Caledonian hotspot? *Plant Soil* 403:53–76. <https://doi.org/10.1007/s11104-016-2910-5>
- Jaffré T (1979) Accumulation du manganèse par les Protéacées de Nouvelle-Calédonie. *C R Acad Sci* 285:425–428
- Jaffré T (1980) Etude écologique du peuplement végétal des sols dérivés de roches ultrabasiqes en Nouvelle-Calédonie. In: *Travaux et Documents de l'ORSTOM n°124*. ORMSTOM, Paris
- Jaffré T, Pillon Y, Thomine S, Merlot S (2013) The metal hyperaccumulators from New Caledonia can broaden our understanding of nickel accumulation in plants. *Front Plant Sci* 4:279. <https://doi.org/10.3389/fpls.2013.00279>
- Kachenko AG, Singh B, Bhatia NP, Siegele R (2008) Quantitative elemental localisation in leaves and stems of nickel hyperaccumulating shrub *Hybanthus floribundus* subsp. *floribundus* using micro-PIXE spectroscopy. *Nucl Inst Methods Phys Res B* 266:667–676. <https://doi.org/10.1016/j.nimb.2007.11.053>
- Kazakou E, Dimitrakopoulos PG, Baker AJ, Reeves RD, Trombis AY (2008) Hypotheses, mechanisms and trade-off of tolerance and adaptation to serpentine soils: from species ecosystems to ecosystems level. *Biol Rev* 83:495–508
- Kelly PC, Brooks RR, Dilli S, Jaffré T (1975) Preliminary observations on the ecology and plant chemistry of some nickel accumulating plants from New Caledonia. *Proc R Soc B Biol Sci* 189:69–80
- Krämer U (2010) Metal hyperaccumulation in plants. *Annu Rev Plant Biol* 61:517–534. <https://doi.org/10.1146/annurev-arplant-042809-112156>
- Kukier U, Peters CA, Chaney RL, Angle JS, Roseberg RJ (2004) The effect of pH on metal accumulation in two *Alyssum* species. *J Environ Qual* 33:2090–2102. <https://doi.org/10.2134/jeq2004.2090>
- Küpper H, Lombi E, Zhao FJ, Wieshammer G, McGrath SP (2001) Cellular compartmentation of nickel in the hyperaccumulators *Alyssum lesbiacum*, *Alyssum bertolonii* and *Thlaspi goesingense*. *J Exp Bot* 52:2291–2300. <https://doi.org/10.1093/jexbot/52.365.2291>
- Lambers H, Brundrett MC, Raven JA, Hopper SD (2010) Plant mineral nutrition in ancient landscapes: high plant species diversity on infertile soils is linked to functional diversity for nutritional strategies. *Plant Soil* 334:11–31. <https://doi.org/10.1007/s11104-010-0444-9>
- Lambers H, Hayes PE, Laliberte E, Oliveira RS, Turner BL (2015) Leaf manganese accumulation and phosphorus-acquisition efficiency. *Trends Plant Sci* 20:83–90. <https://doi.org/10.1016/j.tplants.2014.10.007>
- Latham M, Quantin P, Aubert G (1978) Etude des sols de la Nouvelle-Calédonie. ORSTOM, Paris
- Lindsay WL, Norvell WA (1978) Development of a DTPA soil test for zinc, iron, manganese, and copper. *Soil Sci Soc Am J* 42:421–428
- Loneragan JF (1988) Distribution and movement of manganese in plants. In: Graham RD, Hannam RJ, Uren NC (eds) *Manganese in soils and plants*. Springer, Dordrecht
- Manara A, Fasani E, Furini A, DalCorso G (2020) Evolution of the metal hyperaccumulation and hypertolerance traits. *Plant Cell Environ* 43:2969–2986. <https://doi.org/10.1111/pce.13821>
- Marschner H (2002) Mineral nutrition of higher plants. Academic Press, London
- Memon AR, Ito S, Yatazawa M (1979) Absorption and accumulation of iron, manganese and copper in plants in the temperate forest of Central Japan. *Soil Sci Plant Nutr* 25:611–620
- Mesjasz-Przybyłowicz J, Przybyłowicz W, Barnabas A, van der Ent A (2016) Extreme nickel hyperaccumulation in the vascular tracts of the tree *Phyllanthus balgooyi* from Borneo. *New Phytol* 209:1513–1526. <https://doi.org/10.1111/nph.13712>
- Morat P, Jaffré T, Tronchet F, Munzinger J, Pillon Y, Veillon JM, Chalopin M, Birnbaum P, Rigault F, Dagostini G, Tinel J, Lowry PP (2012) Le référentiel taxonomique Florical et les caractéristiques de la flore vasculaire indigène de la Nouvelle-Calédonie. *Adansonia Sér* 3(34):177–219. <https://doi.org/10.5252/a2012n2a1>
- Munzinger J, Morat P, Jaffré T, Gâteblé G, Pillon Y, Rouhan G, Bruy D, Veillon JM, Chalopin M (2022). [continuously updated] FLORICAL: Checklist of the vascular indigenous flora of New Caledonia. <http://www.publishplantnet-project.org/project/florical>. Accessed January 2022
- Nkrumah P, Echevarria G, Erskine PD, van der Ent A (2018) Contrasting nickel and zinc hyperaccumulation in subspecies of *Dichapetalum gelonioides* from Southeast Asia. *Sci Rep* 8:1–15
- Paul ALD, Gei V, Isnard S, Fogliani B, Echevarria G, Erskine PD, Jaffre T, Munzinger J, van der Ent A (2020a) Nickel hyperaccumulation in New Caledonian *Hybanthus* (Violaceae) and occurrence of nickel-rich phloem in *Hybanthus*



- australocaledonicus*. Ann Bot 126:905–914. <https://doi.org/10.1093/aob/mcaa112>
- Paul ALD, Harris HH, Erskine PD, Przybyłowicz W, Meszjasz-Przybyłowicz J, Echevarria G, van der Ent A (2020b) Synchrotron  $\mu$ XRF imaging of live seedlings of *Berkheya coddii* and *Odontarrhena muralis* during germination and seedling growth. Plant Soil 453:487–501
- Perrier N, Amir H, Colin F (2006) Occurrence of mycorrhizal symbioses in the metal-rich lateritic soils of the Koniambo massif, New Caledonia. Mycorrhiza 16:449–458. <https://doi.org/10.1007/s00572-006-0057-6>
- Pillon Y, Hopkins HCF, Rigault F, Jaffré T, Stacy EA (2014) Cryptic adaptive radiation in tropical forest trees in New Caledonia. New Phytol 202:521–530. <https://doi.org/10.1111/nph.12677>
- Pillon Y, Barrabé L, Buerki S (2017) How many genera of vascular plants are endemic to New Caledonia? A critical review based on phylogenetic evidence. Bot J Linn Soc 183:177–198
- Pillon Y, González DA, Randriambanona H, Lowry PP, Jaffré T, Merlot S (2019a) Parallel ecological filtering of ultramafic soils in three distant island floras. J Biogeogr 46:2457–2465. <https://doi.org/10.1111/jbi.13677>
- Pillon Y, Petit D, Gady C, Soubrand M, Joussein E, Saladin G (2019b) Ionomics suggests niche differences between sympatric heathers (Ericaceae). Plant Soil 434:481–489. <https://doi.org/10.1007/s11104-018-3870-8>
- Pillon Y, Hopkins HCF, Maurin O, Epiawalage N, Bradford JC, Rogers ZS, Baker WJ, Forest F (2021a) Phylogenomics and biogeography of Cunoniaceae (Oxalidales) with complete generic sampling and taxonomic realignments. Am J Bot 108:1181–1200
- Pillon Y, Jaffré T, Birnbaum P, Bruy D, Cluzel D, Ducousso M, Fogliani B, Ibanez T, Jourdan H, Lagarde L, Léopold A, Munzinger J, Pouteau R, Read J, Isnard S (2021b) Infertile landscapes on an old oceanic island: the biodiversity hotspot of New Caledonia. Biol J Linn Soc 133:317–341. <https://doi.org/10.1093/biolinean/blaa146>
- Pollard AJ, Powell KD, Harper FA, Smith JAC (2002) The genetic basis of metal hyperaccumulation in plants. Crit Rev Plant Sci 21:539–566. <https://doi.org/10.1080/0735-260291044359>
- Proctor J (2003) Vegetation and soil and plant chemistry on ultramafic rocks in the tropical Far East. Perspect Plant Ecol Evol Syst 6:105–124. <https://doi.org/10.1078/1433-8319-00045>
- Rao TA, Dickison WC (1985) The veinsheath syndrome in Cunoniaceae. I. *Pancheria* Brongn. & Gris. Proc Plant Sci 95:87–94. <https://doi.org/10.1007/BF03053123>
- Reeves RD (2003) Tropical hyperaccumulators of metals and their potential for phytoextraction. Plant Soil 249:57–65. <https://doi.org/10.1023/a:1022572517197>
- Reeves RD, Baker AJM, Borhidi A, Berazain R (1996) Nickel-accumulating plants from the ancient serpentine soils of Cuba. New Phytol 133:217–224. <https://doi.org/10.1111/j.1469-8137.1996.tb01888.x>
- Reeves RD, Baker AJM, Borhidi A, Berazaín R (1999) Nickel hyperaccumulation in the serpentine flora of Cuba. Ann Bot 83:29–38. <https://doi.org/10.1006/anbo.1998.0786>
- Reeves RD, Baker AJM, Jaffré T, Erskine PD, Echevarria G, Ent A (2017) A global database for plants that hyperaccumulate metal and metalloid trace elements. New Phytol 218:407–411. <https://doi.org/10.1111/nph.14907>
- Ryan CG (2000) Quantitative trace element imaging using PIXE and the nuclear microprobe. International Journal of Imaging Systems and Technology 11(4):219–230
- Ryan CG, Jamieson DN (1993) Dynamic analysis: on-line quantitative PIXE microanalysis and its use in overlapped elemental mapping. Nuclear Instruments and Methods in Physics Research Section B: Beam Interactions with Materials and Atoms 77:203–214
- Ryan CG, Cousens DR, Sie, SH, Griffin WL (1990) Quantitative analysis of PIXE spectra in geoscience applications. Nuclear Instruments and Methods in Physics Research Section B: Beam Interactions with Materials and Atoms 49:271–276
- Ryan CG, Kirkham R, de Jonge MD, Siddons DP, van der Ent A, Pagés A, Boesenberg U, Kuczewski AJ, Dunn P, Jensen M, Liu W, Harris H, Moorhead GF, Paterson DJ, Howard DL, Afshar N, Garrovet J, Spiers K, Falkenberg G et al (2018) The Maia detector and event mode. Synchrotron Radiat News 31:21–27. <https://doi.org/10.1080/08940886.2018.1528430>
- Schneider CA, Rasband WS, Eliceiri KW (2012) NIH image to ImageJ: 25 years of image analysis. Nat Methods 9:671–675
- Schroer CG, Boye P, Feldkamp JM, Patommel J, Samberg D, Schropp A, Schwab A, Stephan S, Falkenberg G, Wellenreuther G, Reimers N (2010) Hard X-ray nanoprobe at beamline P06 at PETRA III. Nucl Instrum Methods Phys Res A 616:93–97
- Sharma SS, Dietz KJ, Mimura T (2016) Vacuolar compartmentalization as indispensable component of heavy metal detoxification in plants. Plant Cell Environ 39:1112–1126. <https://doi.org/10.1111/pce.12706>
- Solé VA, Papillon E, Cotte M, Walter P, Susini J (2007) A multiplatform code for the analysis of energy-dispersive X-ray fluorescence spectra. Spectrochim Acta B 62:63–68
- Tylko G, Meszjasz-Przybyłowicz J, Przybyłowicz W (2007a) In-vacuum micro-PIXE analysis of biological specimens in frozen-hydrated state. Nucl Inst Methods Phys Res B 260:141–148
- Tylko G, Meszjasz-Przybyłowicz J, Przybyłowicz W (2007b) X-ray microanalysis of biological material in the frozen-hydrated state by PIXE. Microsc Res Tech 70:55–68
- van der Ent A, Baker AJM, Reeves RD, Pollard AJ, Schat H (2013) Hyperaccumulators of metal and metalloid trace elements: facts and fiction. Plant Soil 362:319–334. <https://doi.org/10.1007/s11104-012-1287-3>
- van der Ent A, Echevarria G, Tibbett M (2016) Delimiting soil chemistry thresholds for nickel hyperaccumulator plants in Sabah (Malaysia). Chemoecology 26:67–82. <https://doi.org/10.1007/s00049-016-0209-x>
- van der Ent A, Callahan DL, Noller BN, Meszjasz-Przybyłowicz J, Przybyłowicz WJ, Barnabas A, Harris HH (2017a) Nickel biopathways in tropical nickel hyperaccumulating trees from Sabah (Malaysia). Sci Rep 7:41861. <https://doi.org/10.1038/srep41861>
- van der Ent A, Cardace D, Tibbett M, Echevarria G (2017b) Ecological implications of pedogenesis and geochemistry of ultramafic soils in Kinabalu Park (Malaysia). Catena 160:154–169

- van der Ent A, Mak R, De Jonge MD, Harris HH (2018a) Simultaneous hyperaccumulation of nickel and cobalt in *Glochidion* cf. *sericeum* (Phyllanthaceae): elemental distribution and speciation. *Sci Rep* 8:9683
- van der Ent A, Przybyłowicz WJ, Jonge MD, Harris HH, Ryan CG, Tylko G, Paterson DJ, Barnabas AD, Kopittke PM, Mesjasz-Przybyłowicz J (2018b) X-ray elemental mapping techniques for elucidating the ecophysiology of hyperaccumulator plants. *New Phytol* 218:432–452. <https://doi.org/10.1111/nph.14810>
- van der Ent A, Echevarria G, Pollard AJ, Erskine P (2019a) X-ray fluorescence ionomics of herbarium collections. *Sci Rep* 9:4746. <https://doi.org/10.1038/s41598-019-40050-6>
- van der Ent A, Ocenar A, Tisserand R, Sugau JB, Echevarria G, Erskine PD (2019b) Herbarium X-ray fluorescence screening for nickel, cobalt and manganese hyperaccumulator plants in the flora of Sabah (Malaysia, Borneo Island). *J Geochem Explor* 202:49–58. <https://doi.org/10.1016/j.gexplo.2019.03.013>
- van der Ent A, Spiers KM, Brueckner D, Echevarria G, Aarts MGM, Montarges-Pelletier E (2019c) Spatially-resolved localization and chemical speciation of nickel and zinc in *Noccaea tymphaea* and *Bornmuellera emarginata*. *Metalomics*. <https://doi.org/10.1039/c9mt00106a>
- Wang YD, Mesjasz-Przybyłowicz J, Tylko G, Barnabas AD, Przybyłowicz W (2013) Micro-PIXE analyses of frozen-hydrated semi-thick biological sections. *Nucl Inst Methods Phys Res B* 306:134–139

**Publisher's note** Springer Nature remains neutral with regard to jurisdictional claims in published maps and institutional affiliations.